Robust Frequency-Adaptive Quadrature Phase-Locked-Loops with Lyapunov-certified Global Stability

Gilberto Pin (iD), Boli Chen (iD), Giuseppe Fedele (iD), Thomas Parisini (iD)

Abstract— **This work describes and compares two phase-locked-loop (PLL) algorithms aimed at tracking a biased si-nusoidal signal with unknown frequency, amplitude and phase, with inherent robustness to dc-offset. The proposed methods endow Quadrature PLLs, renowned for their excellent tracking performance, with frequency-adaptation capability, while pro-viding robust global stability certificates. The large-gain global stability, proven by Lyapunov-like arguments borrowed from adaptive control theory, represents a major benefit compared to conventional PLLs, whose convergence instead can be proven only locally by small-signal analysis or small-gain assumptions. In this connection, the proposed algorithms represent the first frequency-adaptive and DC-bias rejecting PLL-type architec-tures with Lyapunov-certified global stability. When used for signal tracking, the proposed methods are shown to outperform the adaptive observer, especially in noisy conditions. Moreover, they provide more accurate frequency estimates than existent frequency-adaptive PLLs, showing enhanced robustness in facing both phase-noise and measurement perturbations.**

I. INTRODUCTION

The power distribution network is undergoing tremendous changes due to ever increasing penetration of distributed and renewable energy resources. Such a trend poses new chal-lenges due to the increased unpredictability of these new power sources. A microgrid incorporating the renewable distributed energy resources can be operated either in grid-connected mode or in islanded mode. During both modes of operation, monitoring and control of frequency plays a vital role for power quality assessment, for the control and protection of the power grid and also for the synchronization of the microgrid with the main grid [1]. Due to the presence of disturbances and uncertainties in the grid voltage, such as harmonics, noise,

G. Pin is with Electrolux Italia S.p.A., Italy (gilbertopin@alice.it);
B. Chen is with the Dept. of Electronic and Electrical Engineering, University College London, UK. (boli.chen@ucl.ac.uk);
G. Fedele is with the Dept. of Informatics, Modeling, Elec-tronics and System Engineering, University of Calabria, Italy (giuseppe.fedele@unical.it);
T. Parisini is with the Dept. of Electrical and Electronic Engineering, Imperial College London, UK. He's also with the Dept. of Engineering and Architecture, Univ. of Trieste, Italy and with the KIOS Research and Innovation Centre of Excellence, University of Cyprus, Cyprus (t.parisini@gmail.com). This work has been partially supported by the Italian Ministry for Education, University, and Research (MIUR) under the initiative "Departments of Excellence" (Law 232/2016) and in the framework of the 2017 Program for Research Projects of National Interest (PRIN), Grant no. 2017YKXYXJ, and by European Union's Horizon 2020 research and innovation programme under grant agreement No 739551 (KIOS CoE), and by The Royal Society International Exchanges programme, IES\R2\212041.

offsets and imbalances introduced by the instrumentation and nonlinear loads, it is important that the frequency-estimation approach is robust and fast in terms of response speed to ensure reliable estimates of the fundamental frequency.

There is a rich literature on the approaches for estimat-ing parameters of a sinusoidal signal, including amplitude, frequency and phase angle. This estimation task arises in many engineering domains, such as vibration attenuation in mechanical systems, acoustics, electrical power monitoring, signal processing and fault detection. However, in the con-text of power-electrical engineering, the Phase-Locked-Loop (PLL) method and its many variants still represent the most used approaches. A comprehensive overview of common PLL architectures, such as magnitude PLL (MPLL) [2], enhanced PLL (EPLL) [3] and quadrature-PLL (QPLL) [4], can be found in [5]. These modified PLL configurations are devised to address the deficiency of the conventional PLL by mitigating undesired oscillations. To address the DC-offset that usually appears in an electrical signal, the nominal EPLL has been augmented in [6] by an additional outer integrator loop for DC-bias rejection. Moreover, the quadrature signal generation-based PLLs (QSG-PLLs) are also highly popular for grid synchronization [7], [8], [9], [10]. Depending on the technique used for generating the quadrature signal, these PLLs may be further categorized, such as the delay-based PLL [10]. In the literature, QSG units are sometimes also referred to as Orthogonal Signal Generators (OSG). The Frequency Locked-Loop (FLL) of [11], [12], that uses a Second Order Generalized Integrator (SOGI) to implement the OSG, is for instance capable of tracking sinusoidal signals with time-varying frequency and amplitude. Other methods providing frequency-adaptation ability to a PLL can be found in [13] and [14]. The OSG-SOGI structure is also studied in [15], [16], [17], [18] for biased sinusoidal signals. In particular, [16] proposes a third order generalized integrator-based OSG (OSG-TOGI), which is an effective extension of OSG-SOGI for DC-offset rejection.

In spite of the popularity of the PLL techniques, global Lyapunov stability proof is not available for the majority of existing PLLs [19], [20]. Instead, their stability is usually characterized by small-signal analysis, that provides only local stability guarantees, or by averaging analysis, that relies on small-gain assumptions [2], [14], [21] or a large reference frequency [22]. In such cases, the tuning of adaptation gains is subject to unpractical limiting conditions, and badly tuned gains may lead to instability, particularly for large initialization

error or in presence of measurement disturbances. The recent work presented in [23] studies the global stability domains in the design parameter space for type two PLLs. Nevertheless, the PLL architectures described in [23] have neither frequency adaptation capability nor dc-bias rejection. A wide variety of techniques have been proposed in the literature for enhanced stability properties. The adaptive observer [24], [25], [26], [27], [28], [29] and nonlinear adaptive filtering [30], [31] represent the two common tools for the construction of global or semi-global convergent frequency-adaptive algorithms. Despite coming along with appealing global stability proofs, these methods are not widely used in real-world applications, mainly due to their complexity and the lack of an extensive, comparable sample of practical case-studies.

Recently, a globally convergent PLL scheme with frequency-adaptation capability has been developed in [32] by suitably modifying the standard QPLL configuration. To underline the stability property, the said algorithm has been given the name Global QPLL (GQPLL). To distinguish the original algorithm presented in [32] from the successive variants, in the sequel it will be denoted by Ordinary GQPLL (O-GQPLL). The Lyapunov-based analysis depicted in [32] showed that the adaptation gains of the O-GQPLL can be made arbitrarily large in order to achieve a faster convergence rate, while preserving global stability properties. An improved version of the aforementioned O-GQPLL, endowed with robustifying modifications has been proposed in [33] and named R-GQPLL. By introducing a further filtered augmentation, the adaptation law has been made significantly simpler than that of O-GQPLL. It enables the parameter projection operator to be embedded in the adaptation dynamics, yielding enhanced robustness to external perturbations. In this paper, the two GQPLL variants are compared to provide further insight into following aspects: 1) provide a consolidated summary of the advantages of the R-GQPLL formulation over the O-QPLL, 2) provide Lyapunov stability results in a self-contained fashion, 3) suggest parameter tuning guidelines, and 4) show by extended simulations the robustness of the R-GQPLL with respect to a wide range of disturbances, including bounded measurement noise, phase noise, frequency jumps and phase jumps. In particular, this paper for the first time compares the behavior of four methods, namely R-GQPLL, O-GQPLL, EPLL and Adaptive Observer, in presence of phase-noise, that is a critical perturbation known to destabilize classical PLLs.

The paper is organized as follows. The sinusoid estimation problem in presence of measurement bias is formulated in Section II. In Section III, the two GQPLL algorithms are described. Then, the stability analysis in both cases is dealt with in Section IV. Section V provides simulation examples in which the performance of both approaches are compared. Finally, Section VI comes to a conclusion on the basis of the presented work.

II. PROBLEM FORMULATION AND PRELIMINARIES

Let us consider the following sinusoidal signal $s(t)$ in trigonometric form:

$$s(t) = A\sin(\vartheta(t) + \vartheta_0) = a\sin(\vartheta(t)) + b\cos(\vartheta(t))$$
$$\dot{\vartheta}(t) = \omega, \quad \vartheta(0) = 0, \quad t \geq 0 \tag{1}$$

where $\omega \in \mathbb{R}_{>0}$, $A \in \mathbb{R}_{>0}$ and ϑ_0 are unknown frequency, amplitude and the initial phase angle of the sine wave, while $a, b \in \mathbb{R}$ are unknown parameters associated with the nominal amplitude A by $A = \sqrt{a^2 + b^2}$. The present work concerns the design of an estimation algorithm for reconstructing $s(t)$ and for monitoring the fundamental frequency ω from a biased/perturbed measurement

$$y(t) = s(t) + c \tag{2}$$

where $c \in \mathbb{R}$ is an unknown scalar constant (usually referred to as "measurement bias" or "offset").

The following assumption is introduced in this paper.

Assumption 1: The frequency ω of the sinusoidal signal and the measurement bias c are known to belong to the compact intervals $\underline{\omega} \leq \omega \leq \overline{\omega}$ and $\underline{c} \leq c \leq \overline{c}$ with known (finite) lower and upper bounds $\underline{\omega}, \overline{\omega}, \underline{c}, \overline{c} : 0 < \underline{\omega} < \overline{\omega} < +\infty$, $0 < \underline{c} \leq c \leq \overline{c} < +\infty$.

The tracking objective in the unknown-frequency scenario consists in finding the estimates $\hat{s}$ and $\hat{\omega}$ of $s(t)$ and ω, respectively, such that

$$\lim_{t \to +\infty} s(t) - \hat{s}(t) = 0, \qquad \lim_{t \to +\infty} \omega - \hat{\omega}(t) = 0 \tag{3}$$

III. GLOBAL QUADRATURE PLL ARCHITECTURE

Both the O-GQPLL and the R-GQPLL share the same architecture, derived from the QSG-PLL. The said architecture is sketched in Fig. 1, where $\hat{\Omega}(t)$ denotes the estimate of the squared-frequency $\Omega \triangleq \omega^2$. The estimated signal $\hat{y}(t)$ aimed at tracking $y(t)$ is given by

$$\hat{y}(t) = \hat{a}(t)\sin(\hat{\vartheta}(t)) + \hat{b}(t)\cos(\hat{\vartheta}(t)) + \hat{c}_0, \ t \geq 0. \tag{4}$$

where the instantaneous estimated angle $\hat{\vartheta}(t)$ evolves according to $\dot{\hat{\vartheta}}(t) = \sqrt{\hat{\Omega}(t)}$, $t \geq 0$ with initial condition $\hat{\vartheta}(0) = 0$ without loss of generality. To proceed with the analysis, let us introduce the tracking error $e(t) \triangleq y(t) - \hat{y}(t)$ and the lumped parameter $K \triangleq \Omega c$. According to Assumption 1, there exist $\overline{\Omega} \triangleq \overline{\omega}^2$ and $\underline{\Omega} \triangleq \underline{\omega}^2$, $\overline{K} \triangleq \overline{\omega}^2\overline{c}$ and $\underline{K} \triangleq \underline{\omega}^2\underline{c}$, such that $\Omega \in [\underline{\Omega}, \overline{\Omega}]$ and $K \in [\underline{K}, \overline{K}]$. The parameter adaptation laws for the frequency estimate and the bias estimate will take different form for the two GQPLL variants considered in this work, namely the O-GQPLL and R-GQPLL. In the following, both GQPLLs will be presented and analyzed separately to characterize their stability properties. For the sake of notational simplicity, in the sequel we will neglect the explicit dependence from time of the signals and of the time-varying estimated parameters.

Remark 3.1: It is not the goal of the presented work to guarantee that $\hat{a}$ and $\hat{b}$ converge to a and b, neither that they reach constant values; therefore these signals can be viewed as mere internal variables of the algorithm, instead of estimates
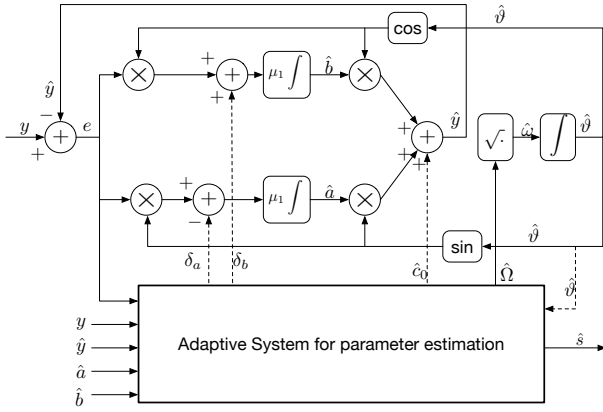
Fig. 1. Scheme of the GQPLL architecture. The dashed lines denote the additional signal paths compared to a conventional QSG-PLL. The Adaptive System block implements different adaptation laws in the two proposed variants: O-GQPLL and R-GQPLL. Together with an estimate of the squared-frequency $\hat{\Omega}$, the Adaptive system injects in the PLL auxiliary signals aimed at achieving robust global stability.

of some time-invariant parameters. This is in line with the requirements of PLL schemes, that are usually required to track a sinusoid, filtering out noise, and, in this case, to estimate its frequency regardless of any measurement offset.

A. Ordinary GQPLL

This Section provides the full algorithm of O-GQPLL. Let us start by introducing the adaptation laws for $\hat{a}$ and $\hat{b}$:

$$\dot{\hat{a}} = \mu_1 \sin(\hat{\vartheta})e - \delta_a , \qquad \dot{\hat{b}} = \mu_1 \cos(\hat{\vartheta})e + \delta_b \qquad (5)$$

where $\mu_1 > 0$ denotes a constant adaptation gain, δ_a and δ_b are two additive signals that do not appear in the conventional QPLL scheme and are injected to enhance the stability of the PLL. These two auxiliary signals are designed as

$$\delta_a \triangleq \sqrt{\hat{\Omega}} \cos(\hat{\vartheta}) \left(\eta_0 \hat{c}_0 + \eta_1 \left(\hat{c}_1 + \sqrt{\hat{\Omega}} \left(\hat{b} \sin(\hat{\vartheta}) - \hat{a} \cos(\hat{\vartheta}) \right) \right) \right) \tag{6a}$$

$$\delta_b \triangleq \sqrt{\hat{\Omega}} \sin(\hat{\vartheta}) \left(\eta_0 \hat{c}_0 + \eta_1 \left(\hat{c}_1 + \sqrt{\hat{\Omega}} \left(\hat{b} \sin(\hat{\vartheta}) - \hat{a} \cos(\hat{\vartheta}) \right) \right) \right) \tag{6b}$$

with two constant tuning parameters $\eta_0 < 0$ and $\eta_1 < 0$ and two internal signals $\hat{c}_0$ and $\hat{c}_1$, that are obtained through the following second-order nonlinear filter, parameterized by a tunable coefficient $\mu_0 > 0$:

$$\dot{\hat{c}}_0 = \hat{c}_1 + \sqrt{\hat{\Omega}} \left(\hat{b} \sin(\hat{\vartheta}) - \hat{a} \cos(\hat{\vartheta}) \right) \tag{7a}$$

$$\dot{\hat{c}}_1 = (\mu_0 - \hat{\Omega})e - \hat{\Omega}\hat{y} + \hat{K}. \tag{7b}$$

Finally, the estimates for the squared-frequency $\hat{\Omega}$ and for the fictitious parameter K are obtained by

$$\hat{\Omega} \triangleq \min \left(\overline{\Omega}, \max \left(\underline{\Omega}, -\frac{k_1}{2} y^2 + \hat{\Theta}_\Omega \right) \right), \tag{8}$$

$$\hat{K} \triangleq \min \left(\overline{K}, \max \left(\underline{K}, k_1 y + \hat{\Theta}_K \right) \right), \tag{9}$$

where

$$\dot{\hat{\Theta}}_\Omega = k_1 y \dot{\hat{y}} - k_0 y e , \qquad \dot{\hat{\Theta}}_K = -k_1 \dot{\hat{y}} + k_0 e . \tag{10}$$

Note that the signal $\dot{\hat{y}}$ needed to implement the above adaptation laws can be obtained from available quantities without direct differentiation:

$$\dot{\hat{y}} = \dot{\hat{a}} \sin(\hat{\vartheta}) + \dot{\hat{b}} \cos(\hat{\vartheta}) + \sqrt{\hat{\Omega}}(\hat{a}\cos(\hat{\vartheta}) - \hat{b}\sin(\hat{\vartheta})) + \dot{\hat{c}}_0$$

$$= \sin(\hat{\vartheta}) \left(\mu_1 \sin(\hat{\vartheta})e - \delta_a \right) + \cos(\hat{\vartheta}) \left(\mu_1 \cos(\hat{\vartheta})e + \delta_b \right) + \dot{\hat{c}}_1 .$$

The expressions (8) and (9) for the estimated squared-frequency and the coefficient K are provided of a saturation that keeps the estimates within the admissible sets. All in all, the adaptive system has a total dynamical order of 7 with states $\hat{\Theta}_k, \hat{\Theta}_\Omega, \hat{c}_0, \hat{c}_1, \hat{a}, \hat{b}, \hat{\vartheta}$, and 6 user-defined constant adaptation gains: $\mu_0, \mu_1, \eta_1, \eta_2, k_0, k_1$. The Lyapunov stability analysis provided in Section IV will be instrumental to derive tuning rules for the said gains in order to boost the performance while maintaining the global stability of the O-GQPLL.

B. Robustified GQPLL

As it can be noticed in Section III-A, the frequency estimation of the O-GQPLL is based on a non-conventional adaptation law, which makes it difficult to apply robustifying modifications of adaptive control. Moreover, the parameter adaptation law given in (8) and (9) involves a direct feedthrough from the noisy measurement y, which tends to increase noise sensitivity. To further improve the robustness of the O-GQPLL while maintaining the global asymptotic convergence property, the dynamics of the PLL internal signals are modified, and make it possible to obtain a convenient first order error model linear-in-the parameters, which can be dealt with by a conventional non-normalized adaptive law. As a consequence, a robustifying modification such as projection can be applied to the adaptive system. The resulting PLL scheme is named Robustified GQPLL (R-GQPLL).

The R-GQPLL differs from O-GQPLL in the parameter-adaptation dynamics. Consider an auxiliary signal y_1, that is obtained by filtering the signal measurement with the following first order low-pass filter:

$$\dot{y}_1 = -\lambda_1 y_1 + y \tag{11}$$

with $\lambda_1 > 0$ an arbitrary positive constant and initial condition $y_1(0) = \overline{y}_1$. Given the filtered output y_1, the signal $\hat{c}_1$ in the R-GQPLL is generated by the following o.d.e.:

$$\dot{\hat{c}}_1 = (\mu_0 - \hat{\Omega})e - \hat{\Omega}\hat{y} + \hat{K} - y_1 \dot{\hat{\Omega}} + \lambda_1^{-1} \dot{\hat{K}}, \ t \geq 0, \tag{12}$$

while the signals $\hat{a}$, $\hat{b}$, $\hat{c}_0$ and $\hat{c}_1$ follow the same dynamics of the O-GQPLL, i.e. (7a) and (5), with a specific choice for the adaptation gains μ_1 and μ_0:

$$\mu_0 \triangleq \lambda_0 \lambda_1, \qquad \mu_1 \triangleq \lambda_0 + \lambda_1, \tag{13}$$

where $\lambda_0 > 0$ is a positive design parameter. The nonlinear signals δ_a and δ_b are constructed by (6) as described in Section III-A, whilst η_0 and η_1 in the case of the R-GQPLL become time-varying signals, that depend on the estimated squared-frequency $\hat{\Omega}$ and its time derivative:

$$\eta_0 = 1 - \mu_0 \frac{1}{\hat{\Omega}}, \qquad \eta_1 = -\mu_1 \frac{1}{\hat{\Omega}} - \frac{\dot{\hat{\Omega}}}{2\hat{\Omega}^2} \tag{14}$$

The division-by-zero singularity in (14) is avoided by constraining $\hat{\Omega}$ in a suitable admissible set. The update laws for $\hat{\Omega}$ and $\hat{K}$ in the case of the R-GQPLL take the following form:

$$
\dot{\hat{\Omega}} = \begin{cases} -k_0 y_1 e, & \begin{cases} (\underline{\Omega} < \hat{\Omega} < \overline{\Omega}) \vee ((\hat{\Omega} = \underline{\Omega}) \wedge (\dot{\hat{\Omega}} > 0)) \\ \vee ((\hat{\Omega} = \overline{\Omega}) \wedge (\dot{\hat{\Omega}} < 0)) \end{cases} \\ 0, & \text{otherwise} \end{cases}
$$
(15)

$$
\dot{\hat{K}} = \begin{cases} \lambda_1^{-1} k_0 e, & \begin{cases} (\underline{K} < \hat{K} < \overline{K}) \vee ((\hat{K} = \underline{K}) \wedge (e > 0)) \\ \vee ((\hat{K} = \overline{K}) \wedge (e < 0)) \end{cases} \\ 0, & \text{otherwise} \end{cases}
$$
(16)

with $k_0 > 0$ the adaptation gain and where the projection operator is utilized to confine $\hat{\Omega}$ and $\hat{K}$ to the admissible convex set specified by the known bounds $\overline{K}, \underline{K}, \overline{\Omega}, \underline{\Omega}$.

Overall, the dynamic order of the R-GQPLL is 8 with an additional dynamic state of the filtered signal y_1 as compared to the O-GQPLL, introduced previously in Section III-A. However, the number of design parameters is halved (only 3 parameters λ_0, λ_1, k_0) that significantly reduces the tuning complexity and makes the design much more straightforward. Moreover, it will be shown that the R-GQPLL admits a greatly simplified stability analysis as compared to the O-GQPLL.

IV. STABILITY ANALYSIS

This Section addresses the stability properties of both GQPLL schemes. To carried out the analysis, following parameter-estimation error variables are defined: $\tilde{\Omega} \triangleq \Omega - \hat{\Omega}$ and $\tilde{K} \triangleq K - \hat{K}$. Let us consider $\theta = [\Omega \ K]^\top$ the parameter vector and denote by $\hat{\theta} \triangleq [\hat{\Omega} \ \hat{K}]^\top$ its estimate. Then, the parameter-estimation error vector is defined as $\tilde{\theta} \triangleq \theta - \hat{\theta}$.

A. Stability Analysis of the O-GQPLL

In view of (8)-(10), when the saturation is disabled, the dynamics of the $\hat{\Omega}$ and $\hat{K}$ are governed by

$$
\dot{\hat{\Omega}} = -k_1 y \dot{y} + k_1 y \dot{\hat{y}} - k_0 y e = -k_1 y \dot{e} - k_0 y e
$$

$$
\dot{\hat{K}} = k_1 \dot{y} - k_1 \dot{\hat{y}} + k_0 e = k_1 \dot{e} + k_0 e
$$

whilst $\dot{\hat{\Omega}} = 0$ and $\dot{\hat{K}} = 0$ when the saturation is active. The estimation error dynamics of both variables accounting for the saturation can be formally expressed by the following differential equations with discontinuous right-hand side (whose solutions are intended in Filippov's sense [34]):

$$
\dot{\tilde{\Omega}} = \begin{cases} k_1 y \dot{e} + k_0 y e, & \begin{cases} (\underline{\Omega} < \hat{\Omega} < \overline{\Omega}) \vee ((\hat{\Omega} = \underline{\Omega}) \wedge (\dot{\hat{\Omega}} > 0)) \\ \vee ((\hat{\Omega} = \overline{\Omega}) \wedge (\dot{\hat{\Omega}} < 0)) \end{cases} \\ 0, & \text{otherwise} \end{cases}
$$
(17)

$$
\dot{\tilde{K}} = \begin{cases} -k_1 \dot{e} - k_0 e, & \begin{cases} (\underline{K} < \hat{K} < \overline{K}) \vee ((\hat{K} = \underline{K}) \wedge (\dot{\hat{K}} > 0)) \\ \vee ((\hat{K} = \overline{K}) \wedge (\dot{\hat{K}} < 0)) \end{cases} \\ 0, & \text{otherwise} \end{cases}
$$
(18)

Now, let us take the time-derivative of the error signal e:

$$
\dot{e} = \omega a \cos(\vartheta) - \omega b \sin(\vartheta) - \dot{\hat{a}} \sin(\vartheta) - \hat{a} \sqrt{\hat{\Omega}} \cos(\hat{\vartheta})
$$
$$
- \dot{\hat{b}} \cos(\hat{\vartheta}) + \hat{b} \sqrt{\hat{\Omega}} \sin(\hat{\vartheta}) - \dot{\hat{c}}_0 \quad (19)
$$

Substituting the expression for $\dot{\hat{c}}_0$ then (19) simplifies into

$$
\dot{e} = \omega a \cos(\vartheta) - \omega b \sin(\vartheta) - \dot{\hat{a}} \sin(\vartheta) - \dot{\hat{b}} \cos(\hat{\vartheta}) - \hat{c}_1 \quad (20)
$$

With reference to the expressions (6) for δ_a and δ_b, (5) can be rewritten as

$$
\dot{\hat{a}} = \mu_1 \sin(\hat{\vartheta}) e - \sqrt{\hat{\Omega}} \cos(\hat{\vartheta}) \left(\eta_0 \hat{c}_0 + \eta_1 \dot{\hat{c}}_0 \right) \quad (21a)
$$

$$
\dot{\hat{b}} = \mu_1 \cos(\hat{\vartheta}) e + \sqrt{\hat{\Omega}} \sin(\hat{\vartheta}) \left(\eta_0 \hat{c}_0 + \eta_1 \dot{\hat{c}}_0 \right) \quad (21b)
$$

where we have exploited the expression for $\dot{\hat{c}}_0$ to streamline the notation. The right hand side of (20) can be further expanded by substituting the expressions (21) for $\dot{\hat{a}}$ and $\dot{\hat{b}}$, respectively

$$
\dot{e} = \omega a \cos(\vartheta) - \omega b \sin(\vartheta) - \mu_1 e - \hat{c}_1 \quad (22)
$$

The second time-derivative of the error yields to:

$$
\ddot{e} = -\Omega(y - c) - \mu_1 \dot{e} - \dot{\hat{c}}_1 \quad (23)
$$

Now, substituting (7b) into (23), after rearrangement with respect to the parameter-estimation error vectors $\tilde{\theta}$, we obtain

$$
\ddot{e} = \xi^\top \tilde{\theta} - \mu_1 \dot{e} - \mu_0 e, \quad (24)
$$

with $\xi = [-y \ 1]^\top$ the vector of regressors. This differential equation will permit to characterize the convergence of the tracking error e and $\tilde{\theta}$. To proceed with the analysis, let us take the second derivative of $\hat{c}_0$:

$$
\ddot{\hat{c}}_0 = \hat{\Omega} \left(\eta_0 \hat{c}_0 + \eta_1 \dot{\hat{c}}_0 \right) + (\mu_0 - \hat{\Omega}) e - \hat{\Omega} \hat{c}_0 + \hat{K}
$$
$$
+ \frac{\dot{\hat{\Omega}}}{2\sqrt{\hat{\Omega}}} \left(\hat{b} \sin(\hat{\vartheta}) - \hat{a} \cos(\hat{\vartheta}) \right) . \quad (25)
$$

By applying the identity $\hat{b} \sin(\hat{\vartheta}) - \hat{a} \cos(\hat{\vartheta}) = (\dot{\hat{c}}_0 - \hat{c}_1)/\sqrt{\hat{\Omega}}$ that is inferred from (7a), (25) can be rearranged, ending up with:

$$
\ddot{\hat{c}}_0 = \hat{\Omega} \left((\eta_0 - 1) \hat{c}_0 + \left(\eta_1 - \frac{k_1 y \dot{e} + k_0 y e}{2 \hat{\Omega}^2} \right) \dot{\hat{c}}_0 \right) + v \quad (26)
$$

where

$$
v \triangleq (\mu_0 - \hat{\Omega}) e + \hat{K}
$$
$$
+ \begin{cases} \dfrac{\hat{c}_1 (k_1 y \dot{e} + k_0 y e)}{2 \hat{\Omega}}, & \begin{cases} (\underline{\Omega} < \hat{\Omega} < \overline{\Omega}) \\ \vee ((\hat{\Omega} = \underline{\Omega}) \wedge (\dot{\hat{\Omega}} > 0)) \\ \vee ((\hat{\Omega} = \overline{\Omega}) \wedge (\dot{\hat{\Omega}} < 0)) \end{cases} \\ 0, & \text{otherwise} \end{cases}
$$
(27)

can be seen as an external input to the above system, depending on the tracking error and on the parameters. The differential equation (25) describes the dynamics of the injection signal $\hat{c}_0$ and will be instrumental to analyze the internal stability of the GQPLL scheme.

Now, we present the stability analysis of the proposed scheme using the Barbalat's Lemma. To apply Barbalat's lemma to the analysis of dynamic systems, we need the following immediate corollary:

Lemma 4.1: (Lyapunov-like Lemma [35]) If a scalar function $V(t, x)$ satisfies the following conditions:

- $V(t, x)$ is lower bounded
- $\dot{V}(t, x)$ is semi-negative definite
- $\dot{V}(t, x)$ is uniformly continuous in time

then $\dot{V}(t,x) \xrightarrow[t\to\infty]{} 0$.

Theorem 4.1: Given the sinusoidal signal $s(t)$ defined in (1) and the biased measurement $y(t)$ (2), the O-GQPLL algorithm given by (5)-(10) guarantees the asymptotic convergence of the tracking error e and of the parameter-estimation error $\tilde{\theta}$, and the boundedness of all the internal signals $\hat{a}$, $\hat{b}$, δ_a, δ_b, $\hat{c}_0$, $\hat{c}_1$.
□

Proof: Consider a dynamic system that collects the parameter-error dynamics (17), (18) and the error system (24) and the dynamics of the auxiliary variable $\hat{c}_0$ (26). The overall system can be viewed as the cascade of two subsystems: 1) the forward system that is described by (17), (18) and (24), and 2) a non-autonomous dynamical system corresponding to the error-driven auxiliary dynamics (26). As such, the overall stability analysis can be performed in two successive steps, respectively, for the two subsystems.

Step A: Consider now the following Lyapunov candidate for the forward system of the error dynamics:

$$V = \frac{1}{2}\left(\overline{e}^\top P \overline{e} + \tilde{\theta}^\top \tilde{\theta}\right)$$

with $\overline{e}^\top \triangleq [e \;\; \dot{e}]^\top$ and the positive definite matrix $P \triangleq \begin{bmatrix} p_{11} & p_{12} \\ p_{12} & p_{22} \end{bmatrix}$. For the sake of the further discussion, let us recast V in the following scalar form $V = p_{11}e^2 + p_{22}\dot{e}^2 + 2p_{12}e\dot{e} + \tilde{\Omega}^2 + \tilde{K}^2$. Given the convexity of the admissible domain for the parameter-estimates $\hat{\Omega}$ and $\hat{K}$, the proposed saturated parameter adaptation law confines the estimate $\hat{\theta} \in \mathbb{R}^2$ within a closed rectangular domain. Thus, it is sufficient to take the conservative route of considering only the unsaturated case [36] to prove the negative-definiteness of the derivative of V along the system's trajectory.

Next, we will show that there exist a $P > 0$, such that V satisfies the assumptions of Lemma 4.1. Considering that $\dot{\tilde{\theta}} = -\dot{\hat{\theta}}$, the derivative of V along the system's trajectory yields:

$$\begin{aligned}
\dot{V} &= p_{11}e\dot{e} + p_{22}\dot{e}\ddot{e} + p_{12}e\ddot{e} + p_{12}\dot{e}^2 - \tilde{\Omega}\dot{\hat{\Omega}} - \tilde{K}\dot{\hat{K}} \\
&= -p_{12}\mu_0 e^2 - (p_{22}\mu_1 - p_{12})\dot{e}^2 + (p_{11} - p_{12}\mu_1 - p_{22}\mu_0)e\dot{e} \\
&\quad + (k_0 - p_{12})\hat{\Omega}ye + (k_1 - p_{22})\hat{\Omega}y\dot{e} \\
&\quad - (k_0 - p_{12})\tilde{K}e - (k_1 - p_{22})\tilde{K}\dot{e}
\end{aligned}$$

To make $\dot{V}$ semi-negative definite, let us first choose arbitrary constant parameters $\mu_0 > 0, \mu_1 > 0$ and $k_0 > 0$ (i.e., there are no small-gain restrictions on the adaptation parameters). Then, pick $p_{12} = k_0$, $p_{22} = \frac{p_{12} + \bar{\mu}_1}{\mu_1}$, for some arbitrary $\bar{\mu}_1 > 0$ and set $k_1 = p_{22}$ and $p_{11} = p_{12}\mu_1 + p_{22}\mu_0$. The positive-definiteness of P descends from the following two facts

$$\begin{aligned}
\det(P) &= p_{22}p_{11} - p_{12}^2 > p_{12}^2 + \bar{\mu}_1 p_{12} - k_0^2 > 0 \\
\mathrm{tr}(P) &= p_{11} + p_{22} > 0
\end{aligned}$$

implying that V is non-negative and radially unbounded. On the other hand, it turns our that $\dot{V}$ is semi-negative-definite:

$$\dot{V} = -k_0\mu_0 e^2 - \bar{\mu}_1 \dot{e}^2 \leq 0$$

with the above choice for the elements of P and the associated design of the tuning parameter. It's easy to show also that $\ddot{V}$ is bounded, implying that $\dot{V}$ is uniformly continuous.

In view of Lemma 4.1, it can be proven that $\overline{e}$ converges to zero. Moreover, in view of well known adaptive control results [37], $\tilde{\theta}$ converges to zero provided the persistency of excitation (PE) of ξ, which is always the case for a sinusoid of nonzero amplitude. Therefore, we can conclude that

$$\lim_{t\to\infty} \hat{y} - y = 0 \implies \lim_{t\to\infty} \hat{y} = s + c, \tag{28a}$$

$$\lim_{t\to\infty} \hat{\Omega} - \Omega = 0 \implies \lim_{t\to\infty} \hat{\Omega} = \omega^2, \tag{28b}$$

$$\lim_{t\to\infty} \hat{K} - K = 0 \implies \lim_{t\to\infty} \hat{K} = \omega^2 c. \tag{28c}$$

Step B: Having already proven that $\lim_{t\to\infty} e = 0$ and $\lim_{t\to\infty} \dot{e} = 0$, it can be inferred from (22) that $\lim_{t\to\infty} \hat{c}_1 = \omega a \cos(\vartheta) - \omega b \sin(\vartheta)$ is bounded. Moreover, the asymptotic convergence of e and $\dot{e}$ also implies that there exists an instant t_ϵ, such that $\eta_1 - \frac{k_1 y\dot{e} + k_0 ye}{2\hat{\Omega}^2} < 0, \forall t > t_\epsilon$ as η_1 is a negative constant. Hence, the dynamics of $\hat{c}_0$ is input-to-state stable (ISS) with respect to v, which is bounded. By inspecting (27), it is immediate to show that $\lim_{t\to\infty} v = \hat{K} = K$, and in turn, from (26), we have that $\lim_{t\to\infty} \hat{c}_0 = \frac{K}{\Omega(1-\eta_0)}$ and $\lim_{t\to\infty} \dot{\hat{c}}_0 = 0$. The previous result combined with (21) implies that $\dot{\hat{a}}$ and $\dot{\hat{b}}$ are bounded. Finally, from (28a), which, along with the boundedness of $\hat{c}_0$, further implies that also $\hat{a}$ and $\hat{b}$ are bounded. Finally, the boundedness of δ_a and δ_b can be proved by invoking (6) and the boundedness of all the aforementioned signals, thus ending the proof.
■

Next, we show that the unbiased sinusoidal signal $s(t)$ (see (1)) can be reconstructed without steady state error by

$$\hat{s} = \hat{y} - \hat{K}/\hat{\Omega}. \tag{29}$$

From the convergence of $\hat{y}$, $\hat{K}$ and $\hat{\Omega}$, it follows that $s - \hat{s} = y - c - \hat{y} + \hat{K}/\hat{\Omega}$ converges to 0 in the steady state. Meanwhile, the convergence of the frequency ω is guaranteed by (28b), and therefore, the objective (3) is achieved.

B. Stability Analysis of the R-GQPLL

Since both GQPLLs have the same adaptation laws for $\hat{a}$, $\hat{b}$, $\hat{c}_0$ and the same definitions of δ_a and δ_b, it is straightforward to show that the second time-derivative of the error signal e in this scenario yet follows (23). By applying expression $\dot{\hat{c}}_1$ shown in (12), the dynamic equation (23) can be expanded as follows:

$$\ddot{e} = -\tilde{\Omega}y + \tilde{K} - \mu_1 \dot{e} - \mu_0 e + y_1 \dot{\hat{\Omega}} - \lambda_1^{-1}\dot{\hat{K}} \tag{30}$$

With reference to the vector of regressors ξ defined in O-GQPLL analysis (see (24)), we now define a vector of filtered regressors $\xi_1 \triangleq [-y_1 \;\; \lambda_1^{-1}]^\top$, evolving according to $\dot{\xi}_1 = -\lambda_1 \xi_1 + \xi$ with initial condition $\xi_1(0) = [-\overline{y}_1 \;\; \lambda_1^{-1}]^\top$, then the tracking-error dynamics (30) can be rearranged and expressed in the following form:

$$\ddot{e} + \mu_1 \dot{e} + \mu_0 e = \xi^\top \tilde{\theta} - \xi_1^\top \dot{\tilde{\theta}} \tag{31}$$

For the sake of brevity, let us denote the Laplace transform of a time-domain signal $u(\cdot): \mathbb{R} \to \mathbb{R}$ by $[\![u]\!](s) = \mathcal{L}\{u(\cdot)\}(s)$.

By applying the Laplace transform to both sides of (31), it holds that

$$(s^2 + \mu_1 s + \mu_0)\llbracket e \rrbracket(s) = \llbracket \xi^\top \tilde{\theta} - \xi_1^\top \dot{\tilde{\theta}} \rrbracket(s) \qquad (32)$$

where the contribution of the exponentially decaying initial conditions have been neglected (the polynomial $s^2 + \mu_1 s + \mu_0$ is Hurwitz by design). From (13), it holds that $s^2 + \mu_1 s + \mu_0 = (s + \lambda_0)(s + \lambda_1)$. As such, equation (32) can be rewritten as

$$\llbracket e \rrbracket(s) = \frac{1}{(s + \lambda_0)(s + \lambda_1)} \llbracket \xi^\top \tilde{\theta} - \xi_1^\top \dot{\tilde{\theta}} \rrbracket(s). \qquad (33)$$

Consider

$$\llbracket e_1 \rrbracket(s) \triangleq \frac{1}{s + \lambda_1} \llbracket \xi^\top \tilde{\theta} - \xi_1^\top \dot{\tilde{\theta}} \rrbracket(s). \qquad (34)$$

The next lines are devoted to show that e_1, in the time domain, verifies

$$e_1 = \xi_1^\top \tilde{\theta}. \qquad (35)$$

By differentiating both sides of (35), we obtain $\dot{e}_1 = -\lambda_1 e_1 + \xi^\top \tilde{\theta} - \xi_1^\top \dot{\tilde{\theta}}$ which is the time-domain equivalent of the Laplace expression (34), thereby (35) is verified. Next, it can be inferred from (33) and (34) that

$$\llbracket e \rrbracket(s) = \frac{1}{s + \lambda_0} \llbracket e_1 \rrbracket(s). \qquad (36)$$

Hence, in the time domain we have the following first order error model

$$\dot{e} = -\lambda_0 e + \xi_1^\top \tilde{\theta}. \qquad (37)$$

which can be dealt with by conventional adaptation laws, such as the projection-based ones given in (15) and (16). Similarly to the analysis performed for the O-GQPLL, let us also introduced the following system that describes the second order time-derivative of $\hat{c}_0$:

$$\ddot{\hat{c}}_0 = \hat{\Omega}\left(\eta_0 \hat{c}_0 + \eta_1 \dot{\hat{c}}_0\right) + (\mu_0 - \hat{\Omega})e - \hat{\Omega}\hat{c}_0 + \hat{K} \\ + \frac{\dot{\hat{\Omega}}}{2\hat{\Omega}}\left(\dot{\hat{c}}_0 - \hat{c}_1\right) - y_1\dot{\hat{\Omega}} + \lambda_1^{-1}\dot{\hat{K}} \qquad (38)$$

Defining $v \triangleq (\mu_0 - \hat{\Omega})e + \hat{K} - \frac{\dot{\hat{\Omega}}}{2\hat{\Omega}^2}\hat{c}_1 - y_1\dot{\hat{\Omega}} + \lambda_1^{-1}\dot{\hat{K}}$ and substituting in (38) the expressions for η_0 and η_1 given in (14), we obtain

$$\ddot{\hat{c}}_0 = -\mu_1 \dot{\hat{c}}_0 - \mu_0 \hat{c}_0 + v. \qquad (39)$$

Theorem 4.2: Given the sinusoidal signal $s(t)$ defined in (1) and the biased measurement $y(t)$ (2), the R-GQPLL algorithm given by (5), (6), (7a), (11)-(16) guarantees the asymptotic convergence of the tracking error e and of the parameter-estimation error $\tilde{\theta}$, and the boundedness of all the other internal signals $\hat{a}, \hat{b}, \delta_a, \delta_b, \hat{c}_0, \hat{c}_1$. $\qquad \square$

Proof: By analogy with the previous analysis of the O-GQPLL, we characterize the stability of the R-GQPLL by resorting to the two-step approach based on the twofold decomposition of the overall adaptive system: 1) the first system is made up of the tracking error dynamics (37) and the parameter-adaptation laws (15) and (16) (that correspond to the time-derivatives of the scalar components of the parameter vector $\hat{\theta}$ and, in turn, of the parameter error vector $\tilde{\theta}$), and 2) the LTI system (39) fed by v, that in turn depends on the tracking error and on the parameter estimates.

Step A): Now, let us introduce the following candidate Lyapunov function for the first subsystem (15), (16) and (37):

$$V = \frac{1}{2}\left(k_0 e^2 + \tilde{\theta}^\top \tilde{\theta}\right) \qquad (40)$$

Similarly to the analysis conducted previously in Section IV-A, it is sufficient to analyze the case in which the projection is non-active.

The derivative of V along the system's trajectory satisfies:

$$\dot{V} = k_0 e\dot{e} - \tilde{\Omega}\dot{\hat{\Omega}} - \tilde{K}\dot{\hat{K}} = -\lambda_0 k_0 e^2 \leq 0$$

From the differential equation (37) we can establish the boundedness of $\dot{e}$ (both $\tilde{\theta}$ and ξ_1 are bounded). Hence both e and $\dot{V}$ are uniformly continuous. By invoking Lemma 4.1, it can be inferred that $\lim_{t\to\infty} e = 0$ and $\tilde{\theta}$ is bounded. Moreover, considering that y is bounded and that, in turn, y_1 is bounded, then from (15) and (16), we have that $\lim_{t\to\infty} \dot{\hat{\theta}} = 0$ (i.e., $\lim_{t\to\infty} \dot{\hat{\Omega}} = 0$ and $\lim_{t\to\infty} \dot{\hat{K}} = 0$). Invoking standard arguments of adaptive control $\tilde{\theta}$ we can conclude that converges to zero (exponentially) in case the regressor's vector ξ_1 is PE, which is always the case for a non-degenerate sinusoid (non-zero amplitude and frequency), which implies (28b) and (28c).

Step B): It remains to prove the boundedness of the auxiliary signals $\delta_a, \delta_b, \hat{c}_0$ and $\hat{c}_1$. From (31) we can conclude that $\ddot{e}$ is bounded, which implies that $\dot{e}$ is uniformly continuous. By Barbalat Lemma we also have that $\lim_{t\to\infty} \dot{e} = 0$. Then, the boundedness of the $\hat{c}_1, \hat{c}_0, \hat{a}$ and $\hat{b}$ can be justified analogously to the analysis carried in the O-GQPLL case. $\qquad \blacksquare$

As a final remark, it is immediate to show the convergence of $\hat{s}$ to s in case of PE by constructing $\hat{s}$ in the form of (29). Hence, the objective (3) is achieved.

Remark 4.1 (Parameter tuning): In view of the stability analysis for both GQPLLs, it turns out that the adaptation gains can be chosen arbitrarily large, enabling faster convergence while preserving global stability properties. The certifiable global stability of the GQPLL out of any small-gain assumption represents a key benefit over the existent frequency adaptive PLL schemes. However, in the presence of the measurement noise, the parameter tuning is subject to the trade-off between asymptotic accuracy and convergence speed. In particular, large k_1 in the O-GQPLL can significantly amplify the noise injection (because of the direct feed-through of y) and degrade asymptotic accuracy. The tuning of R-GQPLL is more straightforward than that of O-GQPLL. It is possible to use a relatively small λ_0 for enhanced noise attenuation (due to the low-pass filter (11)), in conjunction with a large k_0 to compromise the downscale of the signal input to the parameter estimator, and therefore, fast convergence can be preserved without significantly sacrificing the steady state accuracy.

Remark 4.2: Note that the Parameter projection is not mandatory to ensure the boundedness $\hat{a}$ and $\hat{b}$: their boundedness can be inferred from that of other signals. The only parameters for which the projection is required (or other robustifying provisions not considered in this paper, such as σ-modification or deadzone-modification) are $\hat{\Omega}$ and $\hat{K}$, that appear in the Lyapunov function (40), whose time-derivative along system's trajectories is only semi-negative definite.

V. SIMULATION RESULTS

In this Section, the behaviour of proposed GQPLLs will be examined and compared with two representative approaches: the EPLL [6] and an adaptive observer (AO) [38]. In particular, the EPLL is one of the most popular PLL architectures in the electrical applications, while the AO is often taken as a baseline for comparison by the system-theoretic literature.

Example 1: Let us consider a sinusoidal measurement, subjected to sudden frequency and offset variations and a bounded measurement disturbance: $y(t) = c(t) + 300 \sin(2\pi f(t) t) + d(t)$ with $f(t) = 52.5\,\mathrm{Hz}$, $\forall t \in [0, 0.4)$, $f(t) = 47.5\,\mathrm{Hz}$, $\forall t \in [0.4, 1.5]$ and $c(t) = 6$, $\forall t \in [0, 1)$, $c(t) = -12$, $\forall t \in [1, 1.5]$. $d(t)$ is a random noise with uniform distribution in the interval $[-10, 10]$. For fair comparison, all the algorithms are discretized by the Euler method with identical sampling frequency 1MHz and all the methods are initialized with the same initial frequency 50Hz. The O-GQPLL is tuned with: $\mu_0 = 5e4$, $\mu_1 = 200$, $k_0 = 5e5$, $k_1 = 2e4$, $\eta_0 = -80$, $\eta_1 = -15$, while the R-GQPLL is tuned with: $\lambda_0 = 500$, $\lambda_1 = 250$, $k_0 = 6e9$. Both benchmark approaches are tuned so that all the methods approximately share the same rise-time to the initial frequency value.

The frequency-estimation trends obtained in the simulations are depicted in Fig. 2. The initial transient of the frequency-estimates puts in evidence that all the three methods have a similar convergence speed at startup. As shown in Fig. 2, the frequency change at $t = 0.4$s can be captured by all the methods under concern, with comparable response speed. A remarkable feature of the proposed GQPLL algorithms can be appreciated at time $t = 1$s, when the DC-bias term is suddenly changed. The estimates of the AO and EPLL are severely perturbed whereas the GQPLLs are insensitive to the offset-variation without showing noticeable transients. Moreover, the robustness of the GQPLLs is evident from the accuracy of the estimate at steady state. It is also worth noticing the remarkable improvement of R-GQPLL over O-GQPLL in terms of noise immunity, owing to the structural enhancement of the R-GQPLL.

The reconstructed sinusoids provided by the methods under comparison are depicted in Fig. 3. The unbiased sinusoidal signal $s(t)$ can be tracked by all the methods before the frequency change at $t = 0.4$s. However, the AO is unable to retrack $s(t)$ after the frequency is perturbed, and the distortions increase when more changes are introduced. The other three approaches exhibit very similar synchronizing accuracy at steady state, while the transient response of the EPLL tends to be the fastest.
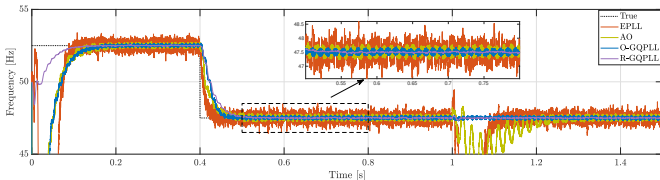

Fig. 2. Frequency estimates provided by the EPLL [6], the AO [38], the O-GQPLL and the R-GQPLL.

Example 2: In this example, the robustness of the proposed methodologies is further verified by more challenging situa-
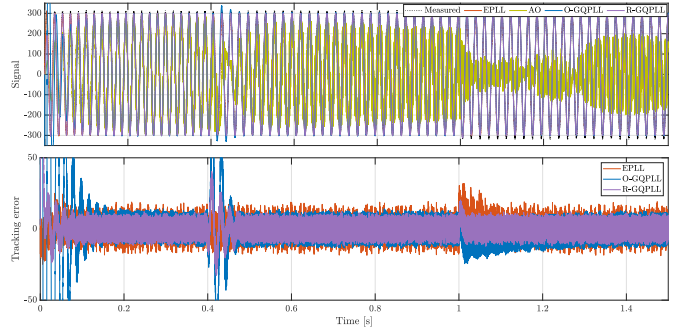

Fig. 3. Tracking performance of EPLL [6], AO [38], the O-GQPLL and the R-GQPLL.

tions. Consider $y(t) = c + 240 \sin(2\pi f t + \Delta \vartheta(t)) + d(t)$ where the frequency and dc offset are fixed, $f = 50\mathrm{Hz}$ and $c = 10$, while the phase angle is perturbed by $\Delta \vartheta(t) = 0$, $\forall t \in [0, 0.4)$, $\Delta \vartheta(t) = \pi/2$, $\forall t \in [0.4, 0.85)$, $\Delta \vartheta(t) = \pi/2 + d_p(t)$, $\forall t \in [0.85, 1.5]$ with $d_p(t)$ a random phase-noise with uniform distribution in the interval $[-0.25, 0.25]$ and $d(t)$ denoting the measurement noise with the same characteristics as in the previous example.

The time behavior of the estimated frequencies provided by all four methods are reported in Fig. 4. As it can be noticed, all the methods succeed in detecting the frequencies with similar initial rising time. The GQPLLs are much less susceptible to an abrupt phase jump, and they can significantly improve the steady steady accuracy even in presence of phase-noise, which severely deteriorates the performance of the EPLL. It is worth noting that the R-GQPLL favorably deals with phase-noise with an almost negligible stationary error. Moreover, the reconstructed sinusoidal signal of each method
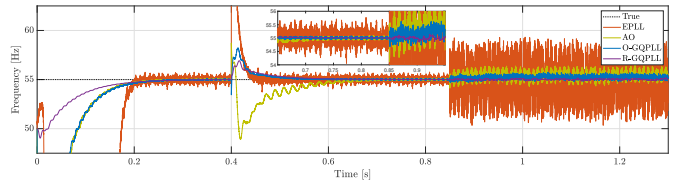

Fig. 4. Frequency estimates provided by the EPLL [6], the AO [38], the O-GQPLL and the R-GQPLL.

are illustrated in Fig. 5 as well as the tracking error. Similarly to the previous example, the AO is less accurate in term of sinusoidal synchronization. Moreover, it follows from Fig. 5
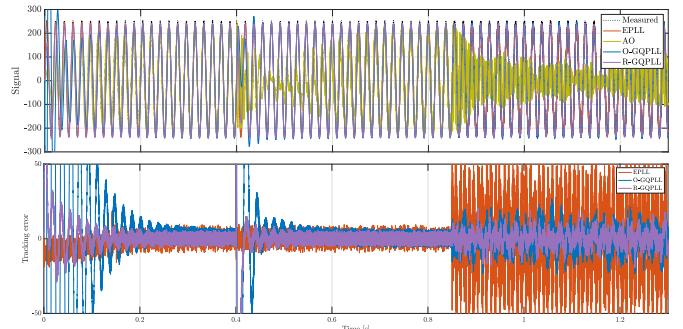

Fig. 5. Tracking performance of EPLL [6], AO [38], the O-GQPLL and the R-GQPLL.

that the GQPLLs are more robust as compared to the EPLL, which is very sensitive to the phase-noise.

VI. CONCLUDING REMARKS

In this paper, the GQPLL paradigm is proposed for robust tracking of a sinusoidal signal and its fundamental frequency in presence of DC offset. Two variants of GQPLL are described: O-GQPLL and R-GQPLL. Both the architectures integrate the conventional OSG-PLL unit with specialized parameter adaptation laws and signal injections. As such, global stability is guaranteed as with adaptive observers, while attaining fast and accurate synchronization to the original sinusoid as required by PLL applications. Moreover, when applied to AC electrical systems, the proposed PLL schemes require only a single-phase sinusoidal measurement for frequency estimation, phase-locking, and fundamental signal reconstruction; therefore, they can be easily extended to three-phase systems without being affected by unbalanced loads.

By comparing the two GQPLLs, the R-GQPLL brings together the fundamental architecture of the O-GQPLL with additional modifications to the internal dynamics that enhance the robustness in presence of unstructured measurement perturbations. Numerical simulations confirm that the R-GQPLL is robust against additive measurement noise and is able to track large and sudden parameter variations. The appealing PLL-like architecture of both the proposed GQPLL schemes together with their certified Lyapunov stability make them a valid alternative to existing PLLs for the task of electrical network monitoring and synchronization with mains.

REFERENCES

[1] S. A. Pourmousavi and M. H. Nehrir, "Real-time central demand response for primary frequency regulation in microgrids," *IEEE Transactions on Smart Grid*, vol. 3, no. 4, pp. 1988–1996, 2012.

[2] B. Wu and M. Bodson, "A magnitude/phase-locked loop approach to parameter estimation of periodic signals," *IEEE Transactions on Automatic Control*, vol. 48, no. 4, pp. 612–618, 2003.

[3] M. Karimi-Ghartemani and A. K. Ziarani, "A nonlinear time-frequency analysis method," *IEEE Transactions on Signal Processing*, vol. 52, no. 6, pp. 1585–1595, 2004.

[4] M. Karimi-Ghartemani, H. Karimi, and M. R. Iravani, "A magnitude/phase-locked loop system based on estimation of frequency and in-phase/quadrature-phase amplitudes," *IEEE Transactions on Industrial Electronics*, vol. 51, no. 2, pp. 511–517, 2004.

[5] S. Golestan, J. M. Guerrero, and J. C. Vasquez, "Single-phase PLLs: A review of recent advances," *IEEE Transactions on Power Electronics*, vol. 32, no. 12, pp. 9013–9030, Dec 2017.

[6] M. Karimi-Ghartemani, S. A. Khajehoddin, P. K. Jain, A. Bakhshai, and M. Mojiri, "Addressing DC component in PLL and notch filter algorithms," *IEEE Transactions on Power Electronics*, vol. 27, no. 1, pp. 78–86, 2012.

[7] M. Mojiri and A. R. Bakhshai, "An adaptive notch filter for frequency estimation of a periodic signal," *IEEE Transactions on Automatic Control*, vol. 49, no. 2, pp. 314–318, 2004.

[8] G. Fedele, C. Picardi, and D. Sgro, "A power electrical signal tracking strategy based on the modulating functions method," *IEEE Transactions on Industrial Electronics*, vol. 56, no. 10, pp. 4079–4087, 2009.

[9] F. Wu, D. Sun, L. Zhang, and J. Duan, "Influence of plugging DC offset estimation integrator in single-phase ePLL and alternative scheme to eliminate effect of input DC offset and harmonics," *IEEE Transactions on Industrial Electronics*, vol. 62, no. 8, pp. 4823–4831, Aug 2015.

[10] S. Golestan, J. M. Guerrero, A. Abusorrah, M. M. Al-Hindawi, and Y. Al-Turki, "An adaptive quadrature signal generation-based single-phase phase-locked loop for grid-connected applications," *IEEE Transactions on Industrial Electronics*, vol. 64, no. 4, pp. 2848–2854, 2017.

[11] G. Fedele and A. Ferrise, "A frequency-locked-loop filter for biased multi-sinusoidal estimation," *IEEE Transactions on Signal Processing*, vol. 62, no. 5, pp. 1125–1134, 2014.

[12] G. Fedele, A. Ferrise, and G. D'Aquila, "A global frequency estimator based on a frequency-locked-loop filter," in *2016 American Control Conference (ACC)*, 2016, pp. 7001–7006.

[13] I. Carugati, P. Donato, S. Maestri, D. Carrica, and M. Benedetti, "Frequency adaptive PLL for polluted single-phase grids," *IEEE Transactions on Power Electronics*, vol. 27, no. 5, pp. 2396–2404, May 2012.

[14] G. Pin, "A direct approach for the frequency-adaptive feedforward cancellation of harmonic disturbances," *IEEE Transactions on Signal Processing*, vol. 58, no. 7, pp. 3523–3530, July 2010.

[15] G. Fedele and A. Ferrise, "Non adaptive second order generalized integrator for identification of a biased sinusoidal signal," *IEEE Transactions on Automatic Control*, vol. 57, no. 7, pp. 1838–1842, 2012.

[16] G. Fedele, A. Ferrise, and P. Muraca, "An adaptive quasi-notch filter for a biased sinusoidal signal estimation," in *IEEE International Conference on Control and Automation (ICCA)*, Santiago, 2011, pp. 1060–1065.

[17] S. Hwang, L. Liu, H. Li, and J. Kim, "DC offset error compensation for synchronous reference frame PLL in single-phase grid-connected converters," *IEEE Transactions on Power Electronics*, vol. 27, no. 8, pp. 3467–3471, Aug 2012.

[18] S. Golestan, M. Monfared, F. D. Freijedo, and J. M. Guerrero, "Design and tuning of a modified power-based PLL for single-phase grid-connected power conditioning systems," *IEEE Transactions on Power Electronics*, vol. 27, no. 8, pp. 3639–3650, Aug 2012.

[19] N. V. Kuznetsov, O. A. Kuznetsova, G. A. Leonov, P. Neittaanmaaki, M. V. Yuldashev, and R. V. Yuldashev, "Limitations of the classical phase-locked loop analysis," in *2015 IEEE International Symposium on Circuits and Systems (ISCAS)*, May 2015, pp. 533–536.

[20] G. A. Leonov, N. V. Kuznetsov, M. V. Yuldashev, and R. V. Yuldashev, "Hold-in, pull-in, and lock-in ranges of pll circuits: Rigorous mathematical definitions and limitations of classical theory," *IEEE Transactions on Circuits and Systems I: Regular Papers*, vol. 62, no. 10, pp. 2454–2464, 2015.

[21] M. Karimi-Ghartemani and M. R. Iravani, "A nonlinear adaptive filter for online signal analysis in power systems: applications," *IEEE Transactions on Power Delivery*, vol. 17, no. 2, pp. 617–622, 2002.

[22] N. V. Kuznetsov, M. Y. Lobachev, M. V. Yuldashev, R. V. Yuldashev, S. I. Volskiy, and D. A. Sorokin, "On the generalized gardner problem for phase-locked loops in electrical grids," *Doklady Mathematics*, no. 103, pp. 157–161, 2021 .

[23] N.V. Kuznetsov, M. Lobachev, M. Yuldashev, and R. Yuldashev, "Analysis of the global stability boundaries in type 2 plls," in *Journal of Physics: Conference Series*, 2021, pp. 1060–1065.

[24] A. A. Bobtsov, N. A. Nikolaev, O. V. Slita, A. S. Borgul, and S. V. Aranovskiy, "The new algorithm of sinusoidal signal frequency estimation," *IFAC Proceedings Volumes*, vol. 46, no. 11, pp. 182 – 186, 2013.

[25] S. Aranovskiy, A. Bobtsov, A. Kremlev, N. Nikolaev, and O. Slita, "Identification of frequency of biased harmonic signal," *European J. of Control*, vol. 16, no. 2, pp. 129 – 139, 2010.

[26] B. Chen, G. Pin, W. M. Ng, C. K. Lee, S. Y. R. Hui, and T. Parisini, "An adaptive observer-based switched methodology for the identification of a perturbed sinusoidal signal: Theory and experiments," *IEEE Transactions on Signal Processing*, vol. 62, no. 24, pp. 6355–6365, 2014.

[27] B. Chen, G. Pin, W. M. Ng, S. Y. R. Hui, and T. Parisini, "An adaptive-observer-based robust estimator of multi-sinusoidal signals," *IEEE Transactions on Automatic Control*, vol. 63, no. 6, pp. 1618–1631, 2018.

[28] G. Pin, Y. Wang, B. Chen, and T. Parisini, "Identification of multi-sinusoidal signals with direct frequency estimation: An adaptive observer approach," *Automatica*, vol. 99, pp. 338 – 345, 2019.

[29] B. Chen, P. Li, G. Pin, G. Fedele, and T. Parisini, "Finite-time estimation of multiple exponentially-damped sinusoidal signals: A kernel-based approach," *Automatica*, vol. 106, pp. 1 – 7, 2019.

[30] G. Pin, B. Chen, T. Parisini, and M. Bodson, "Robust sinusoid identification with structured and unstructured measurement uncertainties," *IEEE Transactions on Automatic Control*, vol. 59, no. 6, pp. 1588–1593, 2014.

[31] B. Chen, G. Pin, W. M. Ng, S. Y. R. Hui, and T. Parisini, "A parallel prefiltering approach for the identification of a biased sinusoidal signal: Theory and experiments," *Int. J. Adaptive Control and Signal Proc.*, vol. 29, no. 12, pp. 1591–1608, 2015.

[32] G. Pin, B. Chen, G. Fedele, and T. Parisini, "Globally-stable tracking and estimation for single-phase electrical signals with dc-offset rejection," in *IECON 2019 - 45th Annual Conference of the IEEE Industrial Electronics Society*, Oct 2019, pp. 4663–4668.

[33] ——, "Robust frequency-adaptive pll with lyapunov stability guarantees," in *Conference on Control Technology and Applications*, 2020.

[34] L. Dieci and L. Lopez, "Sliding motion in filippov differential systems: Theoretical results and a computational approach," *SIAM J. on Numerical Analysis*, vol. 47, no. 3, pp. 2023–2051, 2009.

[35] J.-J. E. Slotine and W. Li, *Applied Nonlinear Control*. Englewood Cliffs, NJ: Prentice Hall, 1991.

[36] E. Lavretsky and T. E. Gibson, "Projection operator in adaptive systems," *ArXiv*, vol. abs/1112.4232, 2012.

[37] B. Anderson and C. Johnson, "Exponential convergence of adaptive identification and control algorithms," *Automatica*, vol. 1, pp. 1–13, 1982.

[38] M. Hou, "Parameter identification of sinusoids," *IEEE Transactions on Automatic Control*, vol. 57, no. 2, pp. 467–472, 2012.